Annual Report of Iwate Medical University
Center for Liberal Arts and Sciences
No. 50(2015), 11-21.

Dual-energy X-ray photon counting using a silicon-PIN diode and its application to photon-count energy subtraction

Eiichi Sato[a], Yasuyuki Oda[a], Satoshi Yamaguchi[b], Osahiko Hagiwara[c], Hiroshi Matsukiyo[c], Manabu Watanabe[c] and Shinya Kusachi[c]

(Accepted July 14, 2015)

Abstract

To obtain two tomograms with two different photon-energy ranges simultaneously, we have performed dual-energy X-ray photon counting using a readymade silicon PIN (Si-PIN) diode, two comparators, two frequency-voltage converters (FVCs), and an analog digital converter (ADC). X-ray photons are detected using the Si-PIN detector with an energy resolution of 3% at 59.5 keV, and the event pulses from a shaping amplifier are sent to two comparators simultaneously to determine two threshold energies of the spectra. The logical pulses from a comparator are sent to an FVC consisting of two integrators, a microcomputer, and a voltage-voltage amplifier. The outputs from the two FVCs are input to a personal computer through the ADC to carry out dual-energy imaging. To observe contrast variations with changes in the threshold energy, we performed dual-energy computed tomography at a tube voltage of 90 kV and a current of 0.68 mA. Two tomograms were obtained simultaneously with two energy ranges of 15-90 and 30-90 keV. The photon-count energy subtraction was carried out using photons with energies ranging from 15 to 30 keV. The maximum count rate for CT was 40 kilo-counts per second with an energy range of 15-90 keV, and the exposure time for tomography was 10 min.

Keywords: dual-energy X-ray photon counting, Si-PIN detector, dual comparator, dual FVC, Gd imaging, photon-count energy subtraction

1. Introduction

To perform monochromatic biomedical radiography, we formed monochromatic cone beams using a single silicon crystal and a conventional X-ray generator [1]. Because the dose rate of this source was low, monochromatic flash X-ray generators [2, 3] have been developed to produce high-dose-rate

[a] Department of Physics, Iwate Medical University, 2-1-1 Nishitokuta, Yahaba, Iwate 028-3694, Japan
[b] Department of Radiology, School of Medicine, Iwate Medical University, 19-1 Uchimaru, Morioka, Iwate 020-0023, Japan
[c] Department of Surgery, Toho University Ohashi Medical Center, 2-17-6 Ohashi, Meguro-ku, Tokyo 153-8515, Japan

clean K-series characteristic rays.

Monochromatic imaging can also be carried out utilizing photon-counting energy-dispersive method, and several energy-dispersive computed tomography (ED-CT) systems [4－7] with cadmium telluride (CdTe) detectors have been developed to perform enhanced K-edge CT using iodine (I) and gadolinium (Gd) contrast media. In particular, although a preclinical ED-CT system [8－10] has been developed using a CdTe-array detector to perform Gd-K-edge CT, fundamental experiments concerning the energy subtraction and the image-quality improvement are also essential in the ED-CT.

Recently, 2-keV-width I-K-edge CT has been performed using a 0.15-keV-resolution silicon PIN (Si-PIN) detector [11], and a 150 kilo-counts per second (kcps) ED-CT has also been carried out using a 2-keV-resolution readymade Si-PIN detector [12] with a comparator to perform Gd-K-edge CT. In addition, a zero-dark-counting CT system with a rate of 200 kcps has also been developed using a detector consisting of a YAP(Ce) (cerium-doped yttrium aluminum perovskite) crystal and an MPPC (multipixel photon counter) [13], since it is not possible to measure X-ray spectra owing to 1-Mcps dark counting using an MPPC module.

Compared with a conventional CT, the image quality of the ED-CT is not good owing to statistical errors. In this regard, a computer program helps smoothing the count rate, but also the smoothing can be carried out using a frequency-voltage converter (FVC) with an integrator.

When we perform two-shot energy subtraction [14] utilizing the ED-CT, both the statistical error and the image granulation increase. Therefore, two-different-energy tomograms should be taken simultaneously, and a dual-energy comparator for performing dual-energy ED-CT is desired to decrease the statistical error.

In our research, major objectives are as follows : to load a readily available Si-PIN diode for energy dispersion, to utilize a dual comparator, to load a developed dual FVC instead of a counter to compensate for the photon-count fluctuations, and to perform photon-count energy subtraction. Therefore, we constructed a dual-energy computed tomography (DE-CT) system with two sets of the comparators and FVCs operated at a tube current of 0.68 mA and performed energy subtraction at a maximum count rate of 40 kcps.

2. Experimental methods

2.1. Dual-energy photon counting

Figure 1 shows a block diagram of dual-energy X-ray photon counting using two sets of the comparators and FVCs. X-ray photons are detected using a readymade Si-PIN diode (Hamamatsu, S5971), and the electric charges produced in the Si-PIN are converted into voltages using charge-sensitive amplifier. The outputs from the charge amplifier are amplified using a shaping amplifier. Subsequently, the event pulses from the shaping amplifier are sent to two comparators simultaneously, and logical pulses from the two comparators are input to the FVCs. The smoothed outputs from the FVCs are sent to a personal computer (PC) through an analog-digital converter.

2.2. DE-CT system

The experimental setup of the CT system is shown in Fig. 2, and the CT system consists of an X-ray generator, a turntable, a scan stage, a two-stage controller, and a dual-energy X-ray photon counting

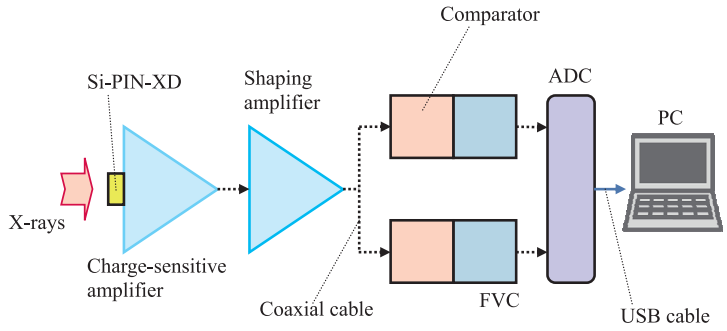

Fig. 1. Block diagram of dual-energy photon counting using a Si-PIN detector and two sets of comparators and FVCs

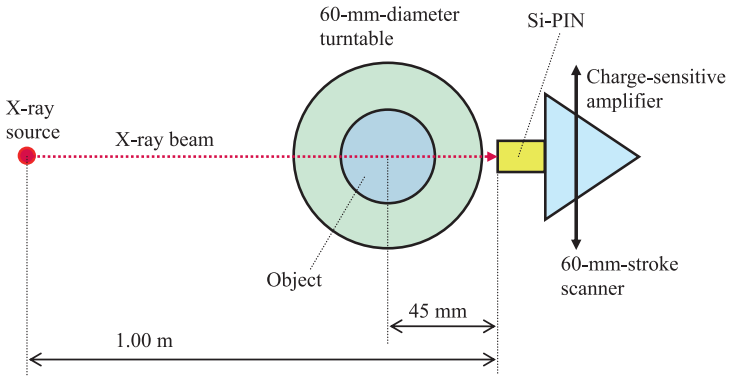

Fig. 2. Experimental setup for performing DE-CT using the Si-PIN detector. The X-ray projection curves for tomography are obtained by repeated linear scans and rotations of the object.

system in Fig. 1. The distance between the X-ray source and the Si-PIN detector is 1.00 m, and the distance from the center of turntable to the detector is 45 mm to decrease magnification ratio of an object. The Si-PIN detector with the charge-sensitive amplifier oscillates on the scan stage with a maximum velocity of 25 mm/s and a stroke of 60 mm. The X-ray projection curves for tomography are obtained by repeated linear scans and rotations of the object, and the scanning is conducted in both directions of its movement. Both scan stage and turntable are driven by the two-stage controller. Two step values of the linear scan and rotation are selected to be 0.5 mm and 1.0°, respectively. Using this CT system, the exposure time is 10 min.

3. Results

3.1. Electric characteristics

Figure 3 shows the time relationship between the microcomputer output and the FVC output. From the microcomputer, the 5.2-V-height 5-μs-width positive logical pulses are produced and are

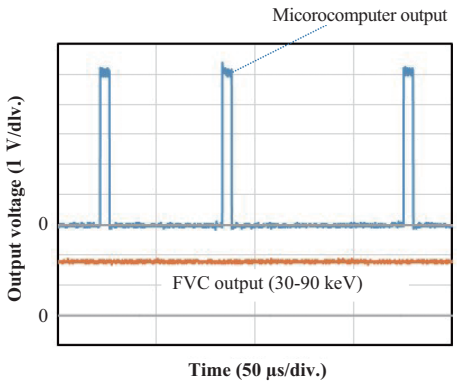

Fig. 3. Time relationship between the microcomputer output and the FVC output.

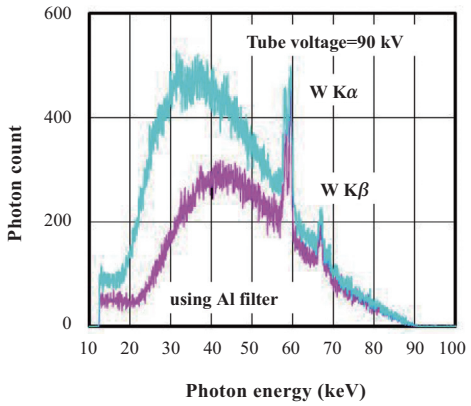

Fig. 4. X-ray spectra measured using a CdTe detector at a tube voltage of 90 kV. The bremsstrahlung peak energy increased with the insertion of an Al filter.

averaged using the first integrator. The integrator output is then amplified using the V-V amplifier with a gain of 20. With energies ranging from 30 to 90 keV and a count rate of 20 kcps, the output voltage from an FVC was 1.8 V.

3.2. X-ray dose rate and spectra

The X-ray dose rate from an X-ray generator was measured using an ionization chamber at a tube current of 0.68 mA without filtration. The chamber was placed 1.0 m from the X-ray source. At a constant tube current, X-ray dose rate increased with increasing tube voltage. At a tube voltage of 90 kV, the X-ray dose rate was 58.3 μGy/s.

X-ray spectra used for CT are shown in Fig. 4. First, we used a CdTe detector with a lead pinhole to measure the standard spectra for reference. According to insertion of a 3.0-mm-thick aluminum (Al) filter, low-energy photons were absorbed, and bremsstrahlung peak energy increased from 35 to 43 keV. The measured spectra using the Si-PIN detector are shown in Fig. 5. Although the detection efficiency of the Si-PIN substantially decreased with increasing energy beyond 40 keV, the maximum energy 90 keV corresponded to the tube voltage of 90 kV. By the Al filtration, the bremsstrahlung peak energy increased. In these spectra, silver (Ag) Kα photons were detected; Ag-Kα fluorescence was produced from the wiring materials in the Si-PIN detector. In the entire spectra with energies ranging from 12 to 90 kV, the maximum count rate was 53 kcps.

The selected X-ray spectra for CT are shown in Fig. 6. Two tomograms were taken simultaneously using two energy ranges of 15-90 keV [Fig. 6(a)] and 30-90 keV [Fig. 6(b)]. Although X-ray photons with energies just beyond Gd-K-edge energy 50.2 keV are useful for imaging Gd atoms, we selected two energy ranges described above to observe contrast variations with changes in the threshold energy and to confirm the subtraction effect. Thus, the average photon energy for CT increases with increasing threshold energy. To reconstruct tomograms with energies ranging from 15 to 30 keV [Fig. 6(c)], photon-

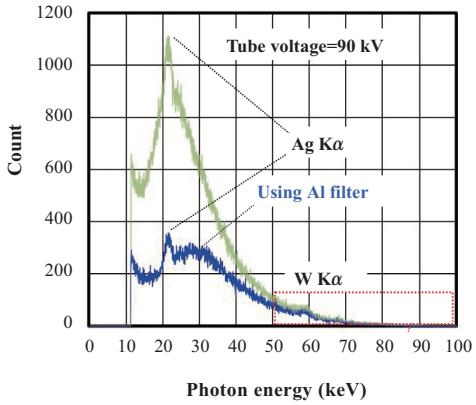

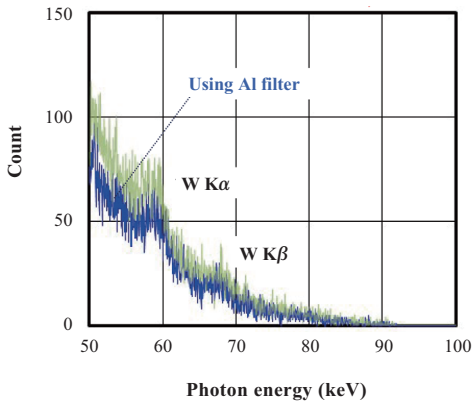

Fig. 5. X-ray spectra measured using a readymade Si-PIN detector at a tube voltage of 90 kV. By the Al filtration, the bremsstrahlung peak energy increased. Although the photon count substantially decreased with increasing energy beyond 40 keV, the maximum energy corresponded to the tube voltage of 90 kV.

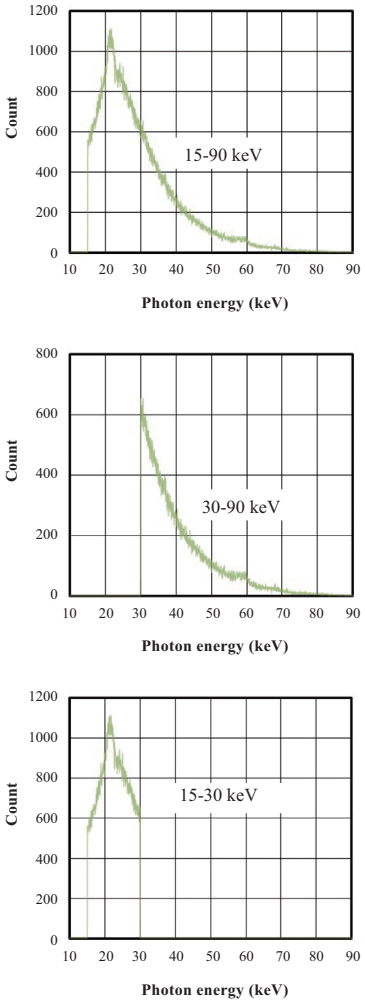

Fig. 6. Selected X-ray spectra for the DE-CT. (a) X-ray photons with energies ranging from 15 to 90 keV, (b) photons with an energy range of 30-90 keV, and (c) photons with an energy range of 15-30 keV selected by photon-count subtraction.

count energy subtraction in the projection curve is used; the photon count is proportional to the FVC output. The count rates of the spectra in Figs. 6(a), 6(b) and 6(c) were 40, 20 and 20 kcps, respectively.

3.3. Tomography

Tomography was performed at a constant tube voltage of 90 kV and a current of 0.68 mA, and the reconstructed maximum and minimum relative photon counts are denoted in black and white, respectively. On the other hand, tomograms are obtained as JPEG files, and the maximum and minimum

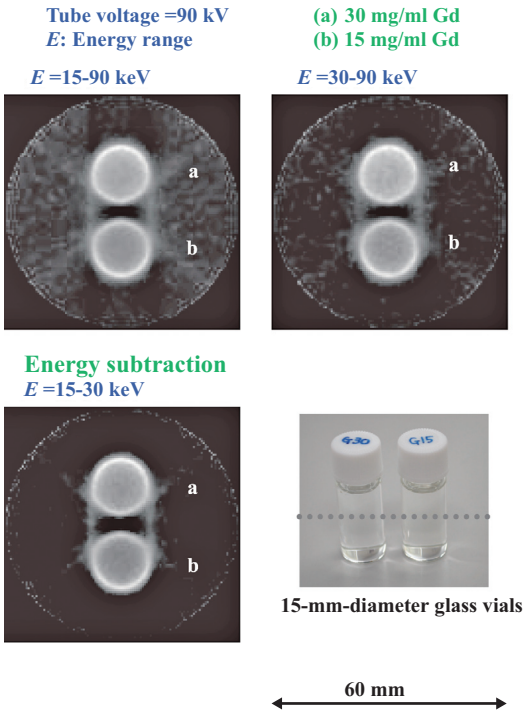

Fig. 7. Tomograms of two 15-mm-diameter glass vials filled with two different density Gd media of 15 and 30 mg/ml. The image densities of the two media slightly increased with increasing threshold energy from 15 to 30 keV. Using photon-count energy subtraction with an energy range of 15-30 keV, the image densities of the Gd media decreased.

gray-value densities are defined as white and black, respectively.

Tomograms of two glass vials filled with Gd media (meglumine gadopentetate) of two different densities 15 and 30 mg/ml are shown in Fig. 7. At a constant maximum energy of 90 keV, the image densities of the two media slightly increased with increasing threshold energy from 15 to 30 keV. The tomogram with energies ranging from 15 to 30 keV was calculated using the photon-count (integrator-output) energy subtraction. Utilizing the subtraction, the image densities of the Gd media decreased.

Figure 8 shows image density analysis of the two vials in Fig. 7 using a computer program Image J. Utilizing energy subtraction, the glass vials were observed at high contrast. Compared with subtraction image, the image densities of the Gd media were high with energies ranging from 30 to 90 keV.

The result of the tomography of a rabbit-head phantom is shown in Fig. 9. The blood vessels were filled with gadolinium oxide (Gd_2O_3) microparticles. The animal experiment was carried out in accordance with the animal experiment guidelines of our university. Radiography (angiography) was performed with a flat-panel detector (FPD; Rad-icon Imaging 1024 EV) to observe blood vessels for reference. In radiography, fine blood vessels were observed because the pixel sizes were $48\times48\ \mu m^2$. At a tube voltage of 90 kV, the image density of muscle slightly decreased with increasing threshold energy from 15 to 30 keV. However, it was difficult to observe the vessels in the subtraction tomogram with

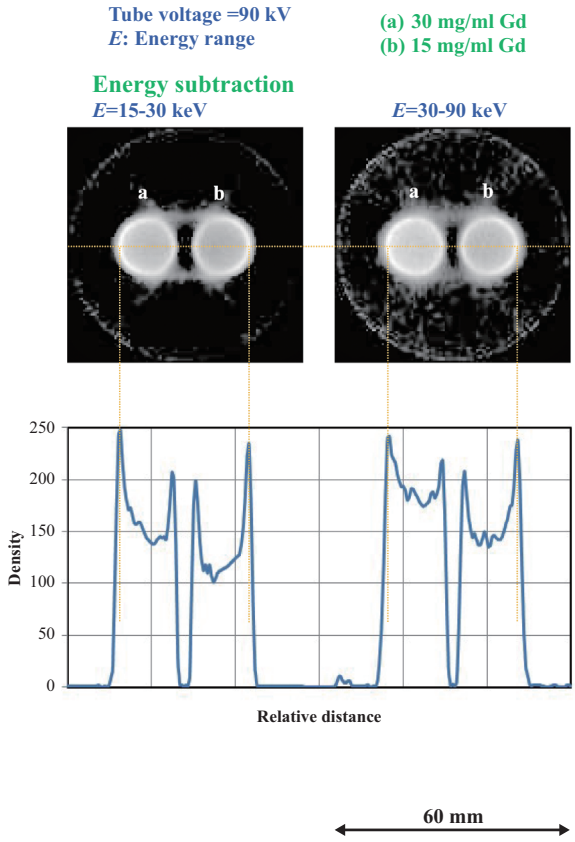

Fig. 8. Image density analysis of the two glass vials in Fig. 7. Using photon-count energy subtraction, the image densities of the two Gd media were lower than those with energies from 30 to 90 keV

energies ranging from 15 to 30 keV.

4. Discussion and conclusions

We performed dual-energy X-ray photon counting using a readily available Si-PIN detector and two sets of comparators and FVCs. In DE-CT, the average photon energy for CT increased with increasing threshold energy from 15 to 30 keV. Using photons with energies ranging from 15 to 90 keV, low-energy CT was performed with a maximum count rate of 40 kcps. Therefore, the maximum count per measuring point was 0.8 kc with a scan step of 0.5 mm and a Si-PIN-scan velocity of 25 mm/s. Next, high-energy CT was accomplished with energies ranging from 30 to 90 keV and a count rate of 20 kcps. Therefore, photon-count energy subtraction was carried out with an energy range of 15-30 keV and a rate of 20 kcps. In addition, the image granulation of the subtraction image was reduced, since the two images were taken simultaneously using the two sets of comparators and FVCs.

Figure 10 shows image density analysis of a glass vial filled with Gd medium with a density of 30 mg/ml. Using a counter card, the image granulation was observed, and the Gd density was quite lower

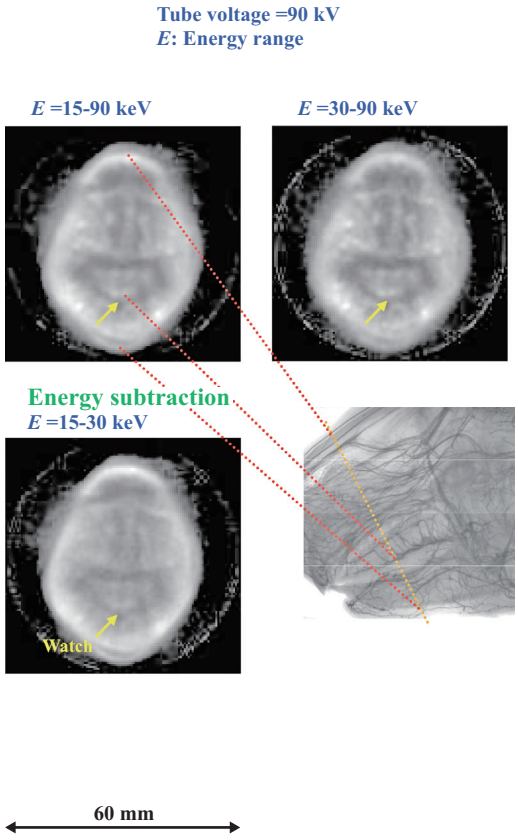

Fig. 9. Tomography of a rabbit-head phantom. The blood vessels were filled with Gd_2O_3 microparticles. With increasing threshold energy from 15 to 30 keV, the image contrasts of the blood vessels were slightly improved. The vessels were not observed at all using energy subtraction.

than that of the glass vial. In addition, the image granulation was also improved using an FVC with two integrators.

In a former experiment using a readymade FVC chip (New Japan Musen, NJM 4151) with an integrator, the output voltage from the integrator was not proportional to the X-ray count rate, because the logical pulse width from the chip slightly decreased with increasing the rate. In the FVC used in this DE-CT, a microcomputer was used to produce constant-width logical pulses, and the integrator output was in proportion to the count rate.

The pixel dimensions of the reconstructed CT image were $0.5 \times 0.5\,mm^2$ because the scan step was 0.5 mm. However, the original spatial resolution is primarily determined by the diameter of the light-receiving surface, and the spatial resolutions were determined as $1.2 \times 1.2\,mm^2$.

In the present work, although we used readily available charge-sensitive and shaping amplifiers, high-count-rate amplifiers should be developed to increase the count rate, to reduce the exposure time for CT, and to decrease the statistical errors. Using these high-rate amplifiers, the maximum rate would

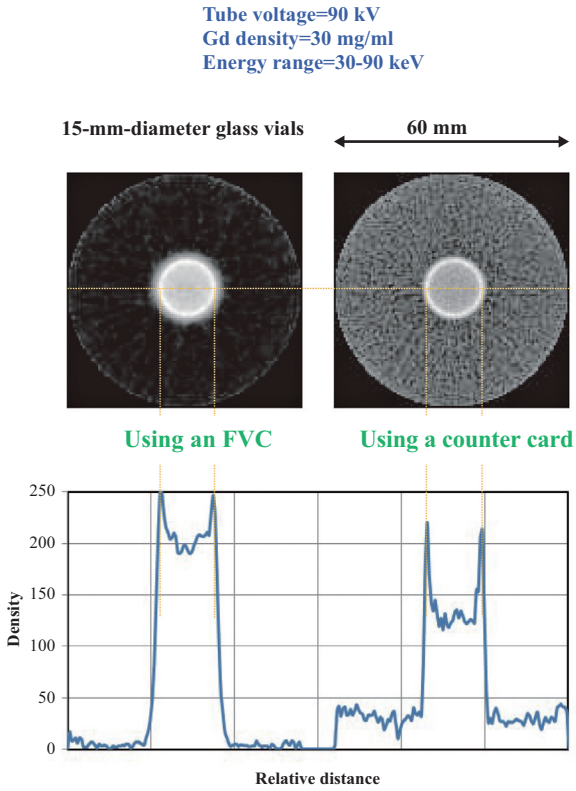

Fig. 10. Image density analysis of a glass vial filled with Gd medium of 30 mg/ml with and without an FVC. Using an FVC, the image granulation was substantially improved.

be increased beyond 200 kcps, and the image quality can be improved.

Using this Si-PIN detector, the detection efficiency substantially decreases with increasing photon energy beyond 40 keV. In view of this situation, because the ED-CT is performed by selecting the photon-energy range, the Gd-K-edge imaging with energies ranging from 50 to 90 keV can be carried out by increasing threshold energy to 50 keV. In addition, it is easy to perform I-K-edge CT with maximum energies ranging from 60 to 70 keV, since it is easy to detect X-ray photons with energies just beyond I-K-edge 33.2 keV.

Acknowledgments

This work was supported by Grants from Keiryo Research Foundation, Promotion and Mutual Aid Corporation for Private Schools of Japan, Japan Science and Technology Agency (JST), and JSPS KAKENHI Grant Number 26461804. We also acknowledged Grant-in-Aid for Strategic Medical Science Research Center from MEXT 2014-2018.

References

[1] Sato, E., Sugiyama, H., Ando, M., Tanaka, E., Mori, H., Kawai, T., Inoue, T., Ogawa, A., Takayama, K., Onagawa, J. and Ido, H., "Tunable narrow-photon-energy x-ray generator utilizing a tungsten-target tube," Rad. Phys. Chem. **75**, 2008-2013 (2006).

[2] Sato, E., Tanaka, E., Mori, H., Kawai, T., Ichimaru, T., Sato, S., Takayama, K. and Ido, H., "Compact monochromatic flash x-ray generator utilizing a disk-cathode molybdenum tube," Med. Phys. **32**, 49-54 (2005).

[3] Sato, E., Hayasi, Y., Germer, R., Tanaka, E., Mori, H., Kawai, T., Inoue, T., Ogawa, A., Sato, S., Takayama, K. and Onagawa, J., "X-ray spectra from weakly ionized linear copper plasma," Jpn. J. Appl. Phys. **45**, 5301-5306 (2006).

[4] Sato, E., Oda, Y., Abudurexiti, A., Hagiwara, O., Matsukiyo, H., Osawa, A., Enomoto, T., Watanabe, M., Kusachi, S., Sato, S., Ogawa, A. and Onagawa, J., "Demonstration of enhanced iodine K-edge imaging using an energy-dispersive X-ray computed tomography system with a 25 mm/s-scan linear cadmium telluride detector and a single comparator," Appl. Rad. Isot. **70**, 831-836 (2012).

[5] Chiba, H., Sato, Y., Sato, E., Maeda, T., Matsushita, R., Yanbe, Y., Hagiwara, O., Matsukiyo, H., Osawa, A., Enomoto, T., Watanabe, M., Kusachi, S., Sato, S., Ogawa, A. and Onagawa, J., "Investigation of energy-dispersive X-ray computed tomography system with CdTe scan detector and comparing-differentiator and its application to gadolinium K-edge imaging," Jpn. J. Appl. Phys. **51**, 102402-1-5 (2012).

[6] Hagiwara, O., Sato, E., Watanabe, M., Sato, Y., Oda, Y., Matsukiyo, H., Osawa, A., Enomoto, T., Kusachi, S. and Ehara, S., "Investigation of dual-energy X-ray photon counting using a cadmium telluride detector and two comparators and its application to photon-count energy subtraction," Jpn. J. Appl. Phys. **53**, 102202-1-6 (2014).

[7] Shimamura, A., Sato, E., Shikanai, S., Kitakami, K., Nakaya, I., Nishikawa, W., Sato, Y., Yamaguchi, S., Oda, Y., Hagiwara, O., Matsukiyo, H., Enomoto, T., Watanabe, M., Kusachi, S. and Ehara, S., "Image-quality improvement in pileup-less cadmium-telluride X-ray computed tomography using a frequency-voltage converter and its application to iodine imaging," Med. Imag. Inform. Sci. **31**, 35-40 (2014).

[8] Feuerlein, S., Roessl, E., Proksa, R., Martens, G., Klass, O., Jeltsch, M., Rasche, V., Brambs, H.J., Hoffmann, M.H.K. and Schlomka, J.P., "Multienergy photon-counting K-edge imaging: potential for improved luminal depiction in vascular imaging," Radiology **249**, 1010-1016 (2008).

[9] Schlomka, J.P., Roessl, E., Dorscheid, R., Dill, S., Martens, G., Istel, T., Bäumer, C., Herrmann, C., Steadman, R., Zeitler, G., Livne, A. and Proksa, R., "Experimental feasibility of multi-energy photon-counting K-edge imaging in pre-clinical computed tomography," Phys. Med. Biol. **53**, 4031-4047 (2008).

[10] Wang, X., Taguchi, K., Frey, E.C., Meier, D., Wagenaar, D.J. and Patt, B.E., "Material separation in x-ray CT with energy resolved photon-counting detectors," Med. Phys. **38**, 1534-1541 (2011).

[11] Hagiwara, O., Watanabe, M., Sato, E., Matsukiyo, H., Osawa, A., Enomoto, T., Nagao, J., Sato, S., Ogawa, A. and Onagawa, J., "Energy-discrimination X-ray computed tomography system utilizing a silicon-PIN detector and its application to 2.0-keV-width K-edge imaging," Nucl. Instr. Meth. A **638**, 165-170 (2011).

[12] Kodama, H., Watanabe, M., Sato, E., Oda, Y., Hagiwara, O., Matsukiyo, H., Osawa, A., Enomoto, T., Kusachi, S., Sato, S. and Ogawa, A., "X-ray photon counting using 100 MHz ready-made silicon P-intrinsic-N X-ray diode and its application to energy-dispersive computed tomography," Jpn. J. Appl. Phys. **52**, 072202-1-6 (2013).

[13] Kami, S., Sato, E., Kogita, H., Numahata, W., Hamaya, T., Nihei, S., Arakawa, Y., Oda, Y., Kodama, H., Hagiwara, O., Matsukiyo, H., Osawa, A., Enomoto, T., Watanabe, M., Kusachi, S., Sato, S. and Ogawa, A., "Zero-dark-counting X-ray photon detection using a YAP(Ce)-MPPC detector and its application to computed tomography using gadolinium contrast media," Rad. Phys. Chem. **100**, 1-7 (2014).

[14] Sato, E., Oda, Y., Abudurexiti, A., Hagiwara, O., Matsukiyo, H., Osawa, A., Enomoto, T., Watanabe, M., Kusachi, S., Sato, S., Ogawa, A. and Onagawa, J., "Demonstration of enhanced iodine K-edge imaging using an energy-dispersive X-ray computed tomography system with a 25 mm/s-scan linear cadmium telluride detector and a single comparator," Appl. Rad. Isot. **70**, 831-836 (2012).